Proceedings of the MEDSI 2014 Conference

Melbourne, Australia - October 2014

Results from Studies of Thermomechanically-Induced Fatigue in GlidCop®

Jeff T. Collins, Jeremy Nudell, Gary Navrotski, Zunping Liu, and Patric Den Hartog
Argonne National Laboratory
9700 S. Cass Avenue, Argonne, IL 60439, U.S.A.

Abstract - GlidCop® is a proprietary dispersion-strengthened copper alloy, most commonly used at hard X-ray third-generation synchrotron facilities to fabricate X-ray absorbers. Thermo-mechanical data and fatigue data for GlidCop® are limited. Although the design criteria limits for X-ray absorbers have been successful in avoiding component failures over the present life of the facility, as the APS and other facilities contemplate upgrades that may result in higher thermal loads on the X-ray absorbers, efforts have been made to establish less conservative, more realistic design criteria limits based on the thermomechanically-induced fatigue limits of GlidCop®. An engineering research program is underway at the APS to determine thermo-mechanical conditions that lead to crack formation and propagation. Using X-ray power from the APS, numerous GlidCop® samples were subjected to 10,000 thermal loading cycles under various beam power conditions and these samples have been metallurgically examined for crack presence/geometry. Temperature-dependent mechanical data and uniaxial fatigue data for GlidCop® have also been obtained from an independent testing facility. Data from these studies support FEA simulation and parametric models so that the thermomechanically-induced fatigue life of X-ray absorbers may be predicted.

Keywords**:** GlidCop®; thermal fatigue life; photon absorbers; high heat load; front ends; design criteria; transient non-linear FEA.

1. Introduction

GlidCop® is a proprietary aluminum oxide dispersion-strengthened copper alloy, and consequently thermo-mechanical data and fatigue data available in the open literature are limited. Hard X-ray third-generation synchrotron facilities commonly use GlidCop® to fabricate X-ray absorbers such as photon shutters, masks and slit assemblies. The existing APS design criteria limits for GlidCop® consider a maximum temperature of 300°C, single-phase cooling water only (no boiling), and a maximum von Mises stress of 400 MPa for photon shutters. Constant room-temperature material properties are used in the linear steady-state FEA. Although the design criteria limits used at the APS for X-ray absorbers have been successful in avoiding component failures over the present life of the facility, as the APS and other facilities contemplate upgrades that may result in higher thermal loads on the X-ray absorbers, efforts have been made to establish less conservative, more realistic design criteria limits based on the thermomechanically-induced fatigue limits of GlidCop® (Ravindranath *et al.*, 2006; Takahashi *et al.*, 2008).

Thermal fatigue is quite different from mechanical fatigue for a number of reasons, one being the presence of inadvertent stress concentration factors in thermal fatigue tests that are absent in mechanical fatigue tests. At a given plastic strain range, thermal fatigue tests will yield fewer cycles to failure than mechanical fatigue tests, even when the upper bound temperature of the thermal fatigue tests does not

exceed the temperature at which the mechanical fatigue tests were conducted (Manson, 1966). However, if plastic strain range is plotted against the number of cycles to failure for the thermal fatigue tests and the mechanical fatigue tests, the slopes of the data sets will be nearly identical. Consequently, a mechanical fatigue model can be used to develop a thermal fatigue model based on observed damage from thermal fatigue tests performed under actual operating conditions.

For this study, several tasks were performed in parallel and used as the basis for the development of a thermal fatigue model for GlidCop® AL-15. Temperature-dependent true stress versus true strain data were obtained for GlidCop® AL-15 in both tension and compression, and this data was used in all transient non-linear FEA performed for this study. Temperature-dependent uniaxial mechanical fatigue data were also obtained for GlidCop® AL-15, and this data was used to develop a mechanical fatigue model. Using X-ray power from the APS, numerous GlidCop® AL-15 test samples were subjected to severe cyclic thermal loading under various beam power conditions, and these test samples have been metallurgically examined for crack presence/geometry. The mechanical fatigue model is then used as the base to develop a thermal fatigue model by matching observed damage with life cycle predictions based on mean temperature. This process allows "failure" to be defined and quantified based on thermal fatigue model predictions and observed damage to the samples.

In addition to the transient non-linear FEA performed on each test sample, used to determine the total strain range and peak temperature data required for the thermal fatigue model, similar analysis was performed on all of the existing APS front end photon shutter designs in order to assess life cycle predictions under various operating conditions. Based upon this analysis, new design criteria limits for GlidCop® AL-15 are proposed, and it is demonstrated how the thermal fatigue model can be used as a tool to geometrically optimize component designs.

2. Mechanical Testing of GlidCop® AL-15

All mechanical tests on GlidCop® AL-15 were performed by an independent testing company, Westmoreland Mechanical Testing & Research, Inc. Temperature-dependent true stress versus true strain data were obtained for GlidCop® AL-15, in both tension and compression, in accordance with ASTM E21-09 and ASTM E209-89a (2000), respectively. Temperature-dependent uniaxial mechanical fatigue data were obtained for GlidCop® AL-15 in accordance with ASTM E606-12. All tests were conducted in a pure argon gas environment. All samples were machined from 12.7 mm x 162 mm GlidCop® AL-15 LOX extruded flat plate, the same material used in many of the APS photon shutter designs for beam strike surfaces.

2. 1. True Stress versus True Strain Testing

Seven different temperatures were chosen for the tests, room temperature and 373K to 873K in 100K increments, and three different samples were tested at each condition. Figure 1 shows the temperature-dependent true stress versus true strain results for tests done in both tension and compression. The true stress vs. true strain test results are similar up to a test temperature of approximately 573K, and at higher temperatures less stress is required to produce the same strain for GlidCop® AL-15 in tension compared to in compression. Data from these tests were curve fit and used in all transient non-linear FEA performed for this study.

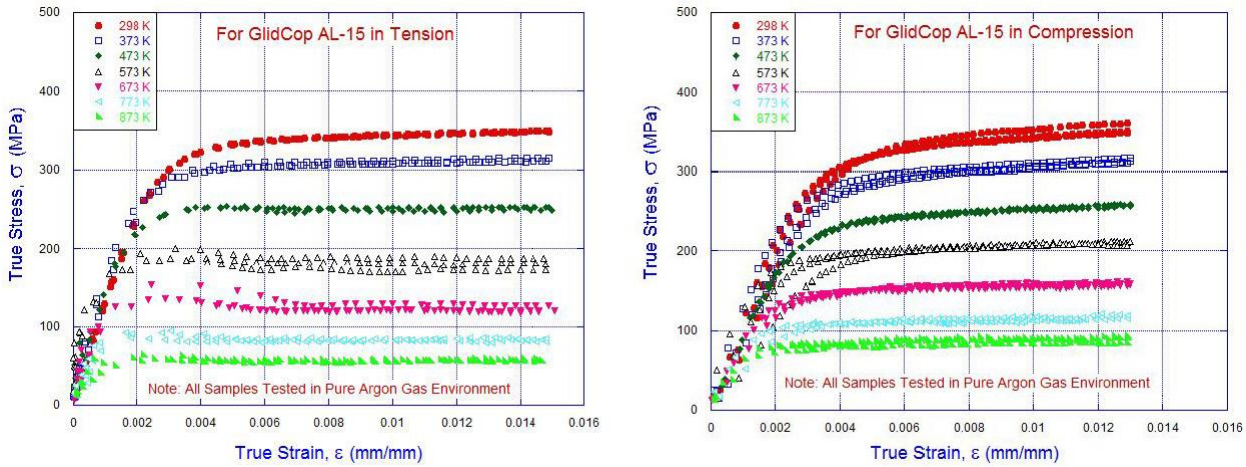

Fig. 1. Temperature-dependent true stress vs. true strain data for GlidCop® AL-15

2. 2. Uniaxial Mechanical Fatigue Testing

Four different temperatures were chosen for the tests, room temperature and 473K to 873K in 200K increments, and total strain ranges were chosen at each test temperature to provide data that would span the range of interest from several hundred cycles to failure up to 20,000 cycles to failure. A total of 45 samples were tested. Linear regression and a method of least squares were used to process the data on the basis of relating the total strain range to the sum of the plastic strain range, approximated by the Manson-Coffin equation (Manson, 1966), with the elastic strain range, approximated by Basquin's law. The exponent for the Manson-Coffin equation, referred to as the fatigue ductility exponent, is derived by plotting the Log of the plastic strain amplitude versus the Log of the number of stress/strain reversals, and then finding a common slope for the four temperature-dependent data sets such that the overall R^2 value, a measure of goodness-of-fit of linear regression, is maximized. Similarly, the exponent for Basquin's law, referred to as the fatigue strength exponent, is derived by plotting the Log of the elastic strain amplitude versus the Log of the number of stress/strain reversals and maximizing the R^2 value. The coefficient for the Manson-Coffin equation, referred to as the fatigue ductility coefficient, is found by using the temperature-dependent y-intercept values from the fatigue ductility exponent data reduction. The coefficient for Basquin's law is the ratio of the fatigue strength coefficient divided by the elastic modulus. Temperature-dependent data for the elastic modulus were obtained from the mechanical fatigue tests conducted by Westmoreland Mechanical Testing & Research, Inc. The fatigue strength coefficient is found by using the temperature-dependent y-intercept values from the fatigue strength data reduction.

The results from the uniaxial mechanical fatigue tests for GlidCop® AL-15 are shown in Figure 2. The mechanical fatigue model is shown at the bottom of the plot where the temperature variable in the equation is the isothermal test temperature. The coefficient for the plastic strain range equation, found to be (2.0 + 3900/T), is the fatigue ductility coefficient. The coefficient for the elastic strain range equation, found to be (.67 – T/2000), is the fatigue strength coefficient divided by the elastic modulus. The solid lines in the plot are the predictions using the mechanical fatigue model for each isothermal test temperature, and it can be seen that good agreement exists between the data and the predictions.

Takahashi (Takahashi *et al.*, 2008) found that the fatigue ductility exponent for the Manson-Coffin equation is dependent upon environmental test conditions. Tests conducted in air yielded a different value than tests conducted in vacuum. In this study, we obtained a value of -0.48 for the fatigue ductility

exponent, identical to the value found by Takahashi, and therefore this suggests that tests performed in a pure argon gas environment yield similar results as tests conducted in vacuum.

The mechanical fatigue model of Figure 2 is transformed into a thermal fatigue model for GlidCop® AL-15 by redefining the temperature variable in the equation as suggested by Taira (Taira, 1973). Whereas the isothermal test temperature is used in the mechanical fatigue model, the mean temperature between the maximum surface temperature and the cooling water temperature is used in the thermal fatigue model. The final equation for the thermal fatigue model for GlidCop® AL-15 is given in Equation 1 where $\Delta\varepsilon_t$ is the total strain range in percent, T_m is the mean temperature in degrees Kelvin, and N_f is the number of cycles to failure.

$$\frac{\Delta\varepsilon_t}{2} = (.67 - \frac{T_m}{2000})(2N_f)^{-.066} + (2.0 + \frac{3900}{T_m})(2N_f)^{-.48} \quad (1)$$

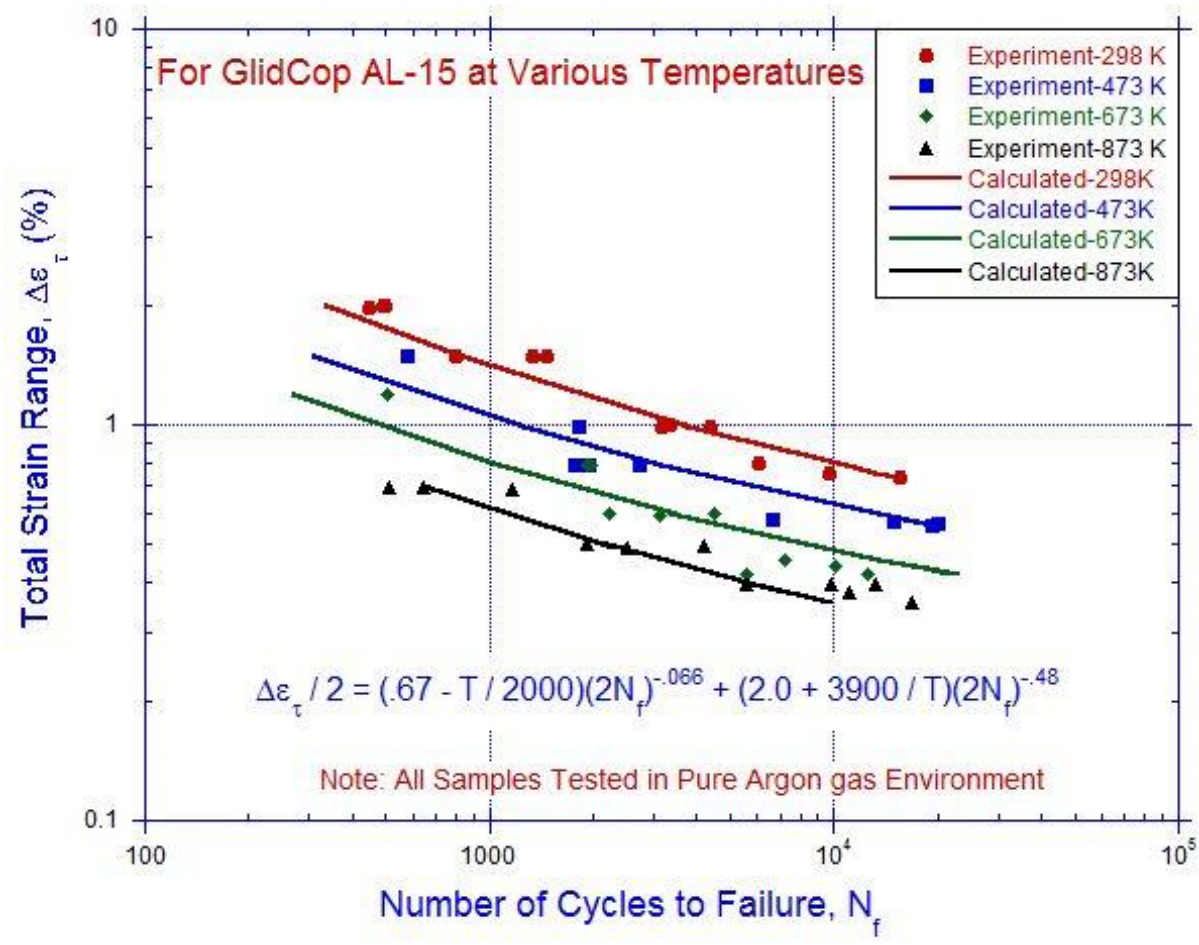

Fig. 2. Temperature-dependent uniaxial mechanical fatigue data for GlidCop® AL-15

3. Thermomechanically-Induced Fatigue Testing of GlidCop® AL-15

3. 1. Experimental Set-Up and Test Sample Configuration

Using X-ray beam delivered from two in-line APS U33.0 undulator-A devices, a total of 30 GlidCop® AL-15 samples were subjected to 10,000 thermal cycles, each at normal incidence, and various beam power loading conditions were applied to the samples. Each test sample assembly consisted of four GlidCop® AL-15 blocks brazed to a common copper cooling tube loop, providing a total of eight test sites. Four sites were provided on one side of the assembly, and then there were four additional sites on the other side when the test sample assembly was rotated 180° inside of the UHV testing chamber. Each sample block measured 101.6 mm L x 27.5 mm H x 22.2 mm W, and the beam strike surfaces were finished to Ra ~ 0.4 µm. The X-ray beam passed through an upstream fixed mask with an aperture size of 4.5 mm x 4.5 mm, and a voice coil-activated photon shutter was used to control the beam exposure cycle time. A cartoon of the experimental set-up is provided in Figure 3.

Prior to the experiments, transient non-linear FEA was performed on a typical test sample in order to determine the required thermal cycle heating and cooling times. In all of the transient non-linear FEA analyses performed for this study, the measured true stress versus true strain data were used in the analysis along with temperature-dependent properties for thermal conductivity, specific heat, thermal expansion coefficient and Young's modulus. It was determined that a 1.4 second heating time and 9 second cooling time is sufficient to achieve near steady-state total strain range, and that peak compressive stress is achieved in less than 0.1 seconds during the heating cycle. The shorter heating and cooling times compared to previous studies (Ravindranath *et al.*, 2006) allowed us to test many more GlidCop® AL-15 samples in the beam time we were allotted to conduct this study.

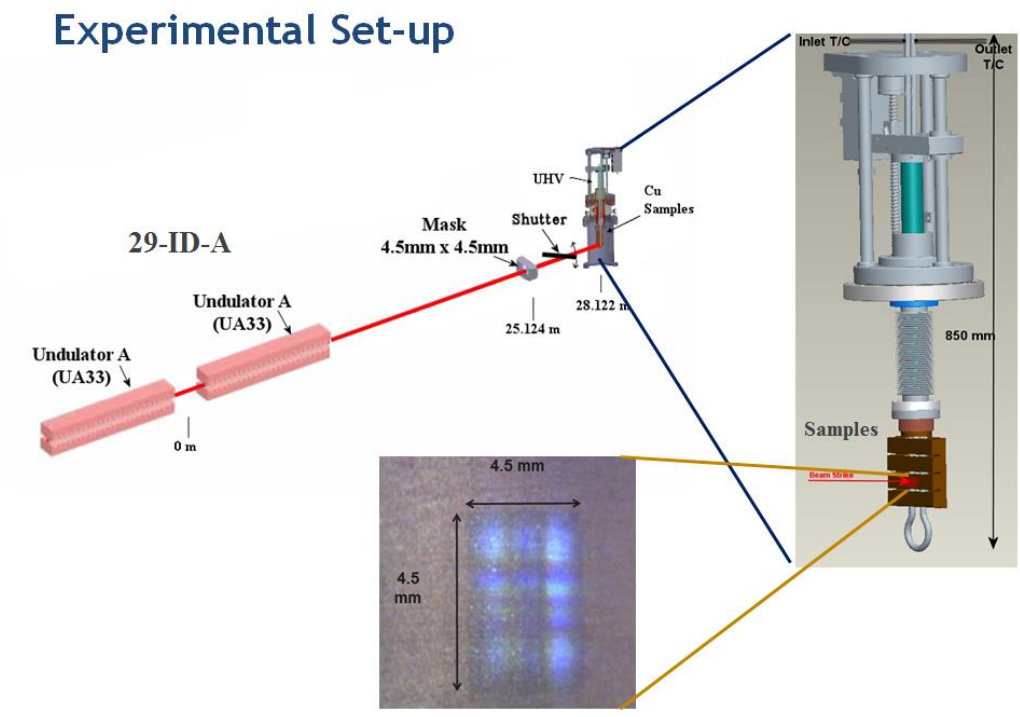

Fig. 3. Experimental set-up for thermomechanically-induced fatigue testing

3. 2. Experimental Results

After 10,000 thermal cycles were applied, surface images were obtained for each GlidCop® AL-15 test sample, and metallurgical sectioning was performed on samples that exhibited crack presence in order to assess crack geometry. Transient non-linear FEA was performed for each load condition in order to determine the total strain range and peak surface temperature, needed to calculate the mean temperature, required to predict the estimated number of cycles to failure based on the thermal fatigue model. Figure 4 provides an example of a typical equivalent stress versus total strain range hysteresis loop obtained from transient non-linear FEA using ANSYS employing the multi-linear kinematic hardening model. If the yield point is exceeded, the strain caused by the first heating cycle plastically deforms the material causing kinematic strain hardening and an increase in yield strength. Only a few thermal cycles are required for the total strain range to converge to a constant value, and therefore only 4 load cycles were required for each simulation.

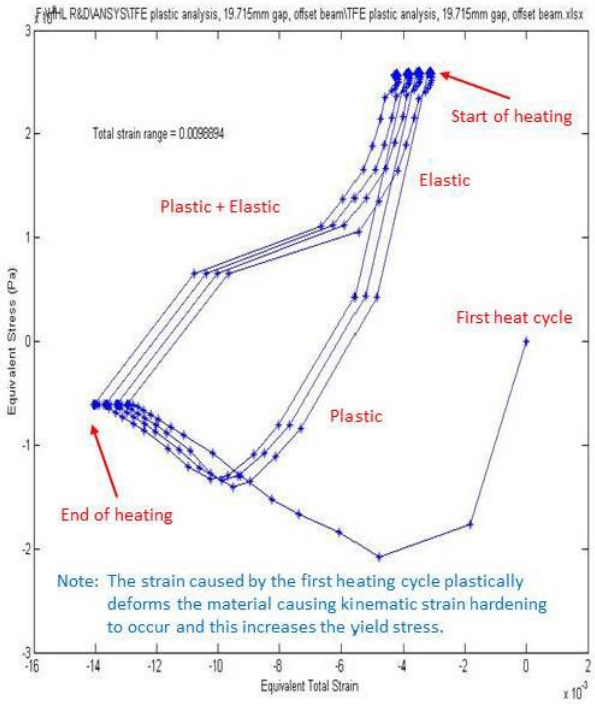

Fig. 4. Typical equivalent stress versus total strain range hysteresis loop

We discovered after testing a number of samples that the beam was offset by 0.53 mm H x 1.18 mm V. The beam was centered for all subsequent sample tests. Calorimetry was performed for both the offset beam cases and the centered beam cases, and the beam location for each sample was accounted for during the transient non-linear FEA. The test sample data base for this study is provided in Table 1 arranged in order of increasing thermal load. Samples highlighted in green are for the cases where the beam is centered whereas samples highlighted in pink are for the cases where the beam was offset. Where applicable, information obtained from metallurgical analysis is provided for the largest crack length, width and depth for each sample. Observations on the sample surface conditions after testing are provided in the comments section. The total strain range for each sample obtained through transient non-linear FEA along with the estimated number of cycles to failure obtained from the thermal fatigue model are also provided.

The red arrow on the right-hand side of Table 1 indicates where the thermal fatigue model predicts 10,000 cycles to failure, and sample groups 1, 2, 3, and 4, indicated on the left-hand side of Table 1, surrounds this point. Samples in group 1 have no surface degradation, whereas samples in groups 2, 3, and 4 have "cat scratches" with the possibility of small, shallow cracks that are less than 2 mm in surface length. "Cat scratches" are shallow regions of surface grain drop-out that are the result of surface thermal compression ejecting weakly bound grains. The GlidCop® AL-15 material is extruded and consequently the copper grains are long and thin, with dimensions on the order of several microns in diameter and tens to hundreds of microns in length, and are aligned in the direction of extrusion. The "cat scratches" observed on sample 10 are shown in Figure 5. Multiple parallel linear "cat scratches" can be seen on several of these samples, and typically one of the "cat scratches" will dominate and provide a site for crack initiation. Based upon the observed damage to

the samples and predictions from the thermal fatigue model, "failure" is defined as "cat scratches" with the possibility of small, shallow cracks less than 2 mm in surface length. This is consistent with the criteria adopted at SPring-8 based upon Japanese industrial standards (Takahashi *et al.*, 2008; JIS Z2279, 1992).

Table. 1. Thermomechanically-induced fatigue in GlidCop® studies sample data base

	Sample Number	Total Absorbed Power, .89 Absorption Coefficient (W)	Peak Heat Flux (W/mm^2)	Total Strain Range (%)	Maximum Temperature , 1.4s heating (K)	Mean Temperature (K)	Largest Crack Length (µm)	Largest Crack Width (µm)	Largest Crack Depth (µm)	Comments	Estimated Number of Cycles to Failure
	37	689.75	101.46	0.40738	685	492				No surface degredation	179,000
	38	689.75	101.46	0.40738	685	492				No surface degredation	179,000
	34	753.83	108.58	0.46806	719	509				No surface degradation	48,100
	35	753.83	108.58	0.46806	719	509				5 "cat scratches"	48,100
1	20	758.28	122.82	0.53048	749	524				No surface degradation	18,100
1	21	758.28	122.82	0.53048	749	524				No surface degradation	18,100
1	22	758.28	122.82	0.53048	749	524				No surface degradation	18,100
1	23	758.28	122.82	0.53048	749	524				No surface degradation	18,100
1	24	758.28	122.82	0.53048	749	524				No surface degradation, 10 stretch marks	18,100
2	32	816.13	115.7	0.53367	752	525				8 small "cat scratches"	17,300
2	33	816.13	115.7	0.53367	752	525	892	47.4	95	Several "cat scratches", 1 small shallow crack	17,300
3	1	817.91	129.94	0.60438	782	540	1815	11	105.8	7 "cat scratches", 5 small shallow cracks	7,650
3	9	817.91	129.94	0.60438	782	540	1238	32.3	235.8	Surface tears, 3 small shallow cracks	7,650
3	10	817.91	129.94	0.60438	782	540	453	11.3		"Cat scratches" and possible cracks	7,650
3	11	817.91	129.94	0.60438	782	540				Many "cat scratches", no cracks	7,650
3	14	877.54	137.06	0.67808	815	557	916	41		Several "cat scratches" and possible cracks	3,880
4	29	881.1	122.82	0.6094	785	542				13 "cat scratches", no cracks	7,220
4	30	881.1	122.82	0.6094	785	542	747	43.4	37	5 "cat scratches", 1 small shallow crack	7,220
4	31	881.1	122.82	0.6094	785	542				>20 "cat scratches" and stretch marks, no cracks	7,220
	6	923.82	142.4	0.73543	840	569	2989	56	630.6	13 "cat scratches", 1 long deep crack, 2 small shallow cracks	2,510
	7	1032.4	153.97	0.86914	897	598	2531	55.9		Many "cat scratches", several long deep cracks	1,110
	4	1141.87	166.43	0.98894	956	627	4329	53	1622	>15 "cat scratches",1 long deep crack	609
	16	1141.87	166.43	0.98894	956	627	3227	224	1218	Many "cat scratches", 1 long deep crack, 4 small shallow cracks	609
	44	1271.81	160.2	1.0487	980	639	2554	117	447.1	Surface "bulging", 2 long deep cracks, 1 small shallow crack	475
	45	1385.73	170.88	1.1464	1034	666				Surface "rumpling", several long deep cracks	320
	46	1385.73	170.88	1.1464	1034	666	4792	34.4		Numerous long deep cracks and melting	320
	43	1508.55	180.67				3623			Numerous long deep cracks and melting	
	41	1783.56	203.81				4624			Numerous long deep cracks and melting	
	42	2092.39	227.84				5269			Numerous long deep cracks and melting	
	47	4679.62	428.09				9668			Numerous long deep cracks and melting	
	Beam offset .53mm H x 1.18mm V										
	Beam centered										

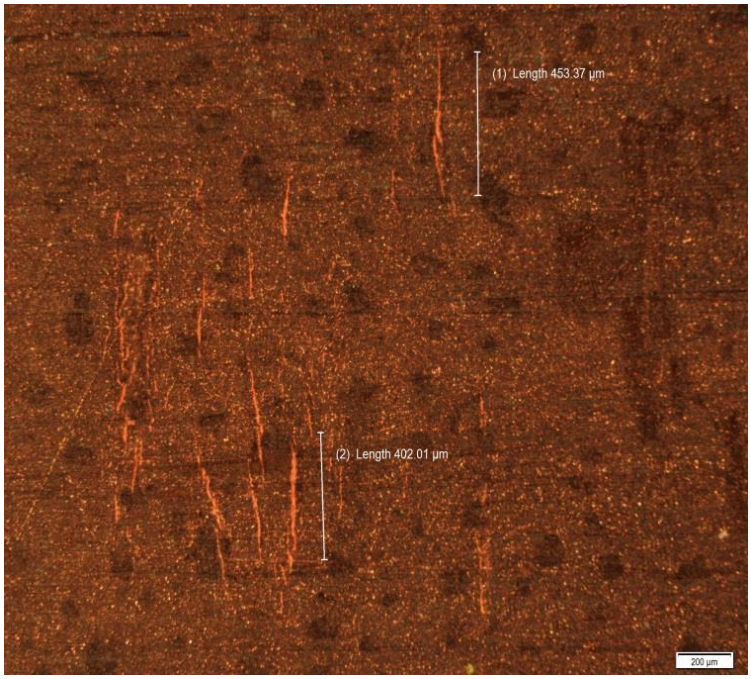

Fig. 5. Typical "cat scratch" pattern caused by surface grain drop-out

4. APS Front End Photon Shutter Transient Non-Linear FEA

Transient non-linear FEA was performed on all of the front end photon shutter designs in operation at the APS, and both the existing maximum design conditions and, where applicable, the maximum MBA lattice baseline conditions planned for the APS Upgrade were considered. It was determined that a 10 second heating time and 40 second cooling time are sufficient to achieve near steady-state total strain range, and that peak compressive stress is achieved in less than a few seconds during the heating cycle.

Table. 2. APS front end photon shutter transient non-linear FEA

Photon Shutter Type	Operating Conditions	Source Parameters	Aperture Size at Shutter Location (mm x mm)	Total Power (W)	Peak Heat Flux (W/mm^2)	Maximum Temperature (°C)	Maximum Cooling Wall Temperature (°C)	Mean Temperature (K)	Peak Compressive / Tensile Stress (Mpa)	Elastic Strain Range (%)	Plastic Strain Range (%)	Total Strain Range (%)	Estimated Number of Cycles to Failure
V1.2 P2-20	Maximum Design Condition from TB-50	Single U33.0 130 mA	9 x 6	6,776	18.0	314.6	147.1	443.0 (169.8°C)	-204.8 / 236.0	0.35786	0.06882	0.42668	152,000
V1.2 P2-20	Water Boiling @ 153°C Condition	Single U33.0 137 mA	9 x 6	7,134	18.9	330.8	153.7	451.1 (177.9°C)	-211 / 250.3	0.36587	0.09170	0.45757	101,000
V1.5 P2-30	Maximum Design Condition from TB-50	Single U33.0 225 mA	9 x 6	11,911	33.4	290.4	94.8	430.9 (157.7°C)	-210.5 / 246.9	0.36629	0.09583	0.46212	114,000
V1.5 P2-30	> 20,000 Cycles to Failure Condition	Dual In-Line U27.5 275 mA	13.48 x 5.52	25,062	36.4	393.4	121.2	482.4 (209.2°C)	-203.6 / 252.1	0.37296	0.10417	0.47713	53,500
PS2 HHL Shutter	Maximum Design Condition from HHL FE Design Report	Dual In-Line U33.0 180 mA	5 x 6	14,600	24.5	248.2	91.9	409.8 (136.6°C)	-205.1 / 173.0	0.30881	0.00615	0.31496	9.57E+06
PS2 HHL Shutter	>20,000 Cycles to Failure Condition	Dual In-Line U27.5 392 mA	5.6 x 6.72	25,527	32.4	375.3	133.3	473.2 (200°C)	-215.4 / 286.6	0.38103	0.17255	0.55358	20,800
PS2 Canted Undulator Shutter	Maximum Design Condition from MEDSI02 Report	Dual Canted U33.0 with 1 mrad Beam Separation 200 mA	10 x 6	19,900	10.4	247.9	129.8	409.6 (136.5°)	-202.4 / 0.0	0.26528	0	0.26528	1.03E+08
PS2 Canted Undulator Shutter	Water Boiling @ 153°C Condition	Dual Canted U27.5 with 1 mrad Beam Separation 330 mA	5.6 x 6.72	20,445	15.9	331.5	153.8	451.4 (178.3°C)	-185.1 / 97.1	0.23395	0	0.23395	3.28E+08

Since time is not a variable in the thermal fatigue model, for each transient simulation, a steady-state thermal simulation was performed first, and the maximum steady-state temperature, required to calculate the mean temperature, was used in the thermal fatigue model. The results from the analyses are presented in Table 2.

Over 20,000 cycles to failure are estimated for all of the cases considered in Table 2. The V1.2 P2-20 photon shutter can only be operated slightly beyond maximum design conditions of 130 mA ring current with a single U33.0 undulator because the water boils at 137 mA. The V1.5 P2-30, the PS2 HHL shutter and the PS2 canted undulator shutter can be operated well beyond the MBA lattice baseline conditions of 200 mA ring current with dual in-line U27.5 undulators. The GlidCop® AL-15 is plastically deformed for all of the cases considered except for the PS2 canted undulator shutter. Here at maximum design conditions of 200 mA ring current with dual canted U33.0 undulators and 1 mradian beam separation, the PS2 canted undulator shutter never enters plasticity, evident by the fact that the peak tensile stress is zero.

The thermal fatigue model can be used to geometrically optimize component designs to reduce cost and component length. Parameters such as cooling wall thickness, grazing incidence angle, cooling channel layout, etc. can be optimized through parametric studies using the thermal fatigue model. This is demonstrated in Table 3 where the grazing incidence angle for the PS2 HHL shutter is incrementally varied from the design angle of 1.05° up to 2.08°. It can be seen that the reduction in life cycle compared to the reduction in shutter length changes significantly between 1.5° and 1.75°, and therefore the optimum grazing incidence angle lies between these angles.

Table. 3. Varying grazing incidence angle for the PS2 HHL shutter

Photon Shutter Type	Operating Conditions	Source Parameters	Grazing Incidence Angle (degrees)	Shutter Length (mm)	Total Power (W)	Peak Heat Flux (W/mm^2)	Maximum Temperature (°C)	Maximum Cooling Wall Temperature (°C)	Mean Temperature (K)	Peak Stress (Mpa)	Elastic Strain Range (%)	Plastic Strain Range (%)	Total Strain Range (%)	Estimated Number of Cycles to Failure
PS2 HHL Shutter	MBA Lattice Baseline Condition	Dual In-Line U27.5 200 mA	1.05	647.7	13,062	16.5	199.3	80.4	385.3 (112.2°C)	-196.9 / 117.5	0.25698	0	0.25698	2.38E+08
PS2 HHL Shutter	MBA Lattice Baseline Condition	Dual In-Line U27.5 200 mA	1.5	556.0	13,063	23.63	276.5	103.1	424.0 (150.8°C)	-199.3 / 193.9	0.33135	0.01847	0.34982	390,000
PS2 HHL Shutter	MBA Lattice Baseline Condition	Dual In-Line U27.5 200 mA	1.75	525.5	13,065	27.57	319.7	115.6	445.6 (172.4°C)	-198.6 / 236.3	0.3604	0.0735	0.4339	37,900
PS2 HHL Shutter	MBA Lattice Baseline Condition	Dual In-Line U27.5 200 mA	2.08	496.4	13,069	32.77	376.5	131.7	473.9 (200.8°C)	-197.0 / 277.5	0.39184	0.14963	0.54147	23,900

5. Proposed New Design Criteria Limits for GlidCop® AL-15

Based upon the results of this study and the transient non-linear FEA performed on all of the APS front end photon shutters, new design criteria limits are proposed for GlidCop® AL-15 as summarized in Figure 6. For most component designs, only steady-state thermal analysis will be required to verify that the design meets the design criteria limits; stress analysis is not required when the maximum surface temperature is 375°C or less. Components can be designed with a maximum surface temperature up to 405°C if transient non-linear FEA is performed to ensure that the number of cycles to failure exceeds 20,000 cycles using the thermal fatigue model. A temperature of 405°C, half the absolute temperature of the GlidCop® AL-15 melting point, is chosen as the maximum since it is the traditional limit where material creep considerations must be included (Manson *et al.*, 2009). The 20,000 cycle limit is chosen since the APS is considering the possibility of re-using some of the older photon shutters for the APS Upgrade. Some of these shutters have been in operation for years and may already have several thousand applied thermal cycles; and therefore, 20,000 cycles to failure is used as a conservative basis. The new design criteria limits also allow for the possibility of designing beyond the boiling point of the water if critical heat flux (CHF) analysis is performed to ensure that a dry-out condition can never be reached. However, at the present, the APS has no plans to pursue this option. Since damage initiation is highly

1. Components can be designed with a maximum surface temperature of 375°C or to where the cooling water will begin to boil; whichever occurs first will be the limiting criteria.

2. Components can be designed with a maximum surface temperature up to 405°C, the creep temperature for GlidCop® AL-15, if transient non-linear analysis is performed to ensure that the number of cycles to failure exceeds 20,000 cycles using the thermal fatigue model below:

$$\frac{\Delta\varepsilon_t}{2} = (.67 - \frac{T_m}{2000})(2N_f)^{-.066} + (2.0 + \frac{3900}{T_m})(2N_f)^{-.48}$$

$\Delta\varepsilon_t$ = Total Strain Range (%)
T_m = Mean Temp. (K) = average of T_{max} & T_{water}
N_f = Number of Cycles to Failure

3. Components can be designed beyond the boiling point of the water if critical heat flux (CHF) analysis is performed to ensure that a dry-out condition can never be reached.

Note: A surface roughness of Ra ≤ 0.4 µm shall be specified for the beam strike surface.

Fig. 6. Proposed new design criteria limits for GlidCop® AL-15

dependent on surface finish, beam strike surfaces shall be designed with a surface roughness of Ra ≤ 0.4 µm, and this can usually be achieved with a double mill pass during machining.

Reviewing the results for the transient non-linear analysis performed on the existing APS photon shutters presented in Table 2, circled in red, it can be seen that the V1.2 P2-20 and PS2 canted undulator photon shutters reach proposed design criteria limits when the cooling water boils. The PS2 HHL shutter reaches design criteria limits when the maximum surface temperature exceeds 375°C with dual in-line U27.5 undulators operating at 392 mA, or when the grazing incidence angle is changed to 2.08° when the maximum MBA lattice baseline conditions planned for the APS Upgrade are applied as shown in Table 3. In all of these cases, the estimated number of cycles to failure is in excess of 20,000 cycles. Using the second design criteria limit, it is shown in Table 2 that by performing transient non-linear FEA and subsequently employing the thermal fatigue model, the V1.5 P2-30 photon shutter can be operated at 275 mA with dual in-line U27.5 undulators and still achieve more than 20,000 cycles to failure with a maximum surface temperature greater than 375°C. Considering the proposed design criteria limits, all of the APS photon shutters can be used in the APS Upgrade except for the V1.2 P2-20 photon shutter. From this analysis, it can be reasoned that a component design could be further optimized by increasing the cooling wall thickness when the limiting design criteria is reaching the boiling point of the cooling water.

The proposed new design criteria limits for GlidCop® AL-15 are intended for flat beam strike surfaces. Consequently, component designs that incorporate stress-concentrating features, such as small radius corners common in fixed mask designs, may achieve a fewer number of cycles to failure.

There is a significant amount of safety built into the new proposed design criteria limits for GlidCop® AL-15. Life-cycle predictions from the thermal fatigue model assume each beam strike occurs under worst-case load conditions at exactly the same spot on the beam strike surface. In reality, as pointed out by Takahashi (Takahashi *et al.*, 2008), damage to the beam strike surface is cumulative, and each load cycle will consume a percentage of the life cycle. Depending on the gap of the undulator(s), many of the load cycles may be far less severe than the worst-case load conditions, and consequently, the number of cycles to failure predicted by the thermal fatigue model may be very conservative.

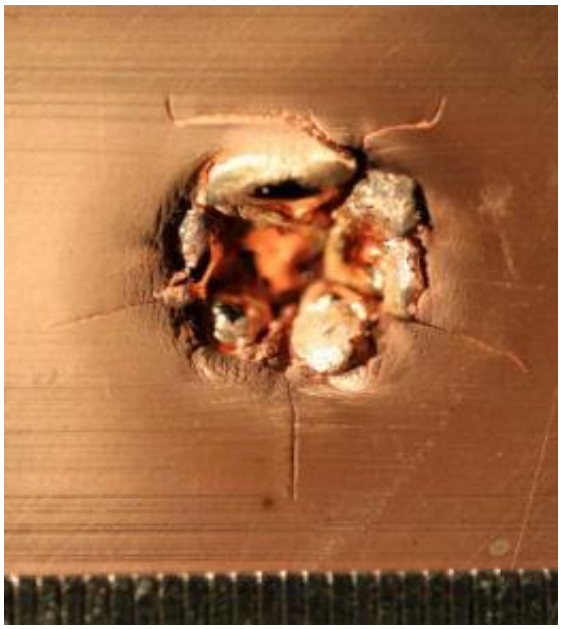

Fig. 7. Sample number 47 tested under worst-case possible beam conditions (1 scale division = 500 µm)

Secondly, sample number 47 received 10,000 thermal cycles under the worst-case possible conditions achievable at the APS using two in-line U33.0 undulators operating at 100 mA maximum storage ring current with closed gaps at 11.0 mm. The total beam power applied was 4,680 W, more than 5.7 times the total beam power applied to the samples in the "cat scratch" region. As shown in Figure 7, although the damage is significant, with evidence of surface extrusion, severe radial cracking, melting and evaporation, the maximum crack length was less than 10 mm and the maximum crack depth was less than 2 mm. Considering the minimum cooling wall thickness for any APS photon shutter design is 6.35 mm, and modern designs use a 9 mm cooling wall thickness, employing the

proposed new design criteria limits for GlidCop® AL-15, it is hard to image a scenario where a crack could ever reach the cooling channel wall.

5. Conclusion

Temperature-dependent true stress versus true strain data and low-cycle mechanical fatigue data were obtained for GlidCop® AL-15. The low-cycle fatigue data were used to develop a temperature-dependent mechanical fatigue model for GlidCop® AL-15 that was then transformed into a thermal fatigue model by appropriately redefining the temperature variable in the model. Numerous GlidCop® AL-15 samples were subjected to 10,000 thermal loading cycles under various beam conditions, and after metallurgical examination, the predictions from the thermal fatigue model for each sample were matched to the observed damage in order to define and quantify "failure". The true stress versus true strain data were curve fit and used in ANSYS along with temperature-dependent mechanical properties to perform non-linear transient FEA on both the test samples and all of the existing APS photon shutter designs in operation at the APS. Based upon the results from this study and the analysis, new design criteria limits for GlidCop® AL-15 are proposed. Furthermore, it is demonstrated how the thermal fatigue model can be used as a tool to geometrically optimize component designs. It is explained how a significant amount of safety is built into the new design criteria limits.

References

JIS Z2279 (1992). Japanese Industrial Standard. *Method of high-temperature low-cycle testing for metallic materials.*

S.S. Manson (1966), Thermal Stress and Low-Cycle Fatigue, McGraw-Hill Book Company, LCCN 65-25918, 131-144 and 255-257.

S.S. Manson and G.R. Halford, Fatigue and Durability, ASM International, LCCN 2009923304, 1-2.

V. Ravindranath, S. Sharma, B. Rusthoven, M. Gosz, L. Zhang, & J. Biasci (2006), *Proceedings of the International Workshop on Mechanical Engineering Design of Synchrotron Radiation Equipment and Instrumentation 2006*, Himeji, Hyogo, Japan.

S. Taira (1973), "Relationship between thermal and low-cycle fatigue at elevated temperatures," *Fatigue at Elevated Temperatures, ASTM STP 520,* American Society for Testing and Materials, 80-101.

S. Takahashi, T. Mochizuki, M. Sano, A. Watanabe, H. Kitamura (2008), "Fatigue life prediction for high-heat-load components made of GlidCop by elastic-plastic analysis," *J. Synchrotron Rad.* (2008). **15**, 144-150.